NURETH14-115

ANALYTICAL AND EXPERIMENTAL ASSESSMENT OF CANDU FUEL SHEATH INTEGRITY UNDER POST DRYOUT CONDITIONS

M.E. Shawkat¹, H. Hasanein¹, T. Daniels², Y. Parlatan², M. Bayoumi¹, and H. Albasha³

¹ Fuel and Fuel Channel Safety Analysis, AMEC-NSS, Ontario, Canada

² Nuclear Safety And Technology Dept., Ontario Power Generation, Ontario, Canada

³ Fuel and Fuel Channel Safety Analysis, Bruce Power, Toronto, Ontario, Canada

Abstract

The experiments that investigated the CANDU fuel sheath behavior under different pressures, temperatures, oxidizing environment, material structure (as-received or thermally treated to attach appendages), and heating rates were reviewed and assessed to determine the limits of post-dryout duration, sheath temperature, and pressure difference across the sheath required to ensure the fuel sheath integrity. A number of burst curves at different heating rates were studied. Time-at-temperature fuel sheath failure maps were developed based on temperature ramp and isothermal experiments for the 28-element fuel bundle. Analytical time-at-temperature fuel sheath failure maps were also developed for both of 28- and 37-element fuel bundles using the ELOCA fuel analysis computer code and were compared to the experimental time-at-temperature sheath failure maps. Time-at-temperature sheath failure maps could be used as a simple and effective screening tool to demonstrate fuel sheath integrity during postulated design basis accident.

Introduction

During Small Break Loss of Coolant Accidents (SBLOCA) and Loss Of Flow (LOF) accidents, prior to reactor trip, the critical heat flux (CHF) could be exceeded and dryout of the fuel sheath could occur. Heat transfer at dryout patches is characterized by a reduced heat transfer coefficient and relatively high local sheath temperatures. Post-dryout operation of the fuel elements at or near their nominal power causes these patches to grow and spread both circumferentially and axially, subjecting the fuel elements to a non uniform heatup. Extended periods of fuel heatup prior to reactor trip could potentially challenge the fuel sheath integrity. Fuel sheath failure could potentially occur due to several mechanisms that depend on post-dryout duration, sheath temperature, and the pressure difference across the sheath (or more generally the sheath hoop stress). These failure mechanisms include sheath failure due to overstrain (high sheath hoop strain), beryllium assisted crack penetration (BACP)¹, and athermal strain. An increase in the sheath temperature causes a decrease in the material strength and when accompanied by an increase in the pressure difference across the sheath (in the outward direction), it could result in elevated sheath strain and eventually sheath failure.

During LOF and SBLOCA accident scenarios, the reactor trip setpoint function is to either prevent or limit the extended dryout duration in order to ensure fuel sheath integrity. Therefore, it

¹ This mechanism is associated with beryllium brazed alloys used to attach fuel element appendages to the sheath outer surfaces. Under high temperatures and sheath stresses, sheath failure may occur at the brazing locations due to liquid metal embrittlement.

is important to experimentally investigate the fuel sheath integrity during post-dryout duration and identify the conditions that can affect the sheath integrity.

In the Canadian nuclear industry all the nuclear power reactors are of CANDU² design. The CANDU fuel bundles currently in use can be broadly classified by the number of the fuel elements in the bundles, into the 28-element and the 37-element fuel bundle types. The fuel sheaths of both bundle types are made of Zircaloy-4 and have the same length and the same sheath thickness range, however, the 28-element fuel bundle has a slightly larger sheath outside diameter than the 37-element fuel bundle (i.e., about 15.25 and 13.08 mm, respectively). To separate the fuel elements from each other and to separate the fuel elements from the fuel channel a number of appendages are brazed onto the outer surface of the fuel sheath. Brazing these appendages to the fuel sheaths alters the metallurgical structure of the fuel sheath in the vicinity of the appendage locations creating what is called the "Heat Affected Zone (HAZ)" region.

The objective of this paper is to specify the limits of post-dryout duration, sheath temperature, and pressure difference across the sheath required to maintain the fuel sheath integrity under post-dryout duration conditions.

1. Review of experimental data

The experimental data that were reviewed in this study to investigate fuel sheath integrity under different conditions and environments are summarized in Table 1. The majority of the experiments used CANDU fuel sheath samples; however, a few non-CANDU fuel sheath samples were also included. All the experiments listed in Table 1 were performed using unirradiated sheaths without fuel pellets. Two main types of experimental procedures have been used to investigate the fuel sheath integrity:

- 1- <u>Temperature ramp experiments:</u> In these experiments, the internal gas pressure inside the specimen is held constant and the sheath is heated (either directly using the sheath sample itself as a heater or indirectly using an external heating element) at a constant rate up to the burst point. However, in some of the experiments, the internal pressure was allowed to vary during the temperature ramp.
- 2- <u>Isothermal holding experiments:</u> In these experiments, the specimen is either pressurized and then heated to a pre-determined temperature or heated to a pre-determined temperature and then pressurized. In both cases, the test specimen was maintained at the pre-determined temperature until it fails (mainly due to creep).

In these experiments, sheath temperatures were measured by soldering thermocouples to the sheath outer surface. The pressure was measured using a gauge either directly by measuring the sheath internal pressure while maintaining the outer pressure constant or differentially across the fuel sheath. To investigate the effect of sheath oxidation, several experiments were conducted in steam. Some of the experiments used as-received Zircaloy-4 samples while other experiments used samples with appendages or samples with HAZ (without having the appendages) to simulate the effect of the metallurgical changes along the CANDU fuel sheath. Most of the experiments that used CANDU fuel samples employed 28-element fuel sheaths. The

² CANDU is a registered trademark of Atomic Energy Canada Limited (AECL).

experimental data for 37-element fuel is sparse and covers limited conditions. The majority of the experiments in Table 1 examined the fuel sheath integrity under uniform temperature conditions. However, temperature gradients due to localized dryout patches could cause sheath failure by overstrain at average strains lower than uniformly heated fuel elements. Williams [1] argued that setting a conservative limit for the sheath overstrain (i.e., 5% criterion used in CANDU reactors) could sufficiently accommodate the reduction in failure strain due to axial and circumferential temperature gradients. This was supported by the experimental data of Rosinger and Ferner [2]. The experimental data considered fuel sheath failures due to sheath overstrain and BACP. Sheath failure due to athermal strain was not observed in these experiments as this mechanism occurs at sheath temperatures lower than the investigated range and requires a high pressure difference to cause sheath failure (as indicated in Sills and Holt [3]).

The experiments clearly indicate that the fuel sheath integrity is a function of the post-dryout duration, sheath temperature, and the pressure difference across the sheath. An excessive difference between the internal gas pressure (P_{gas}) and the coolant pressure ($P_{coolant}$) could cause fuel sheath failure at relatively low temperatures and shorter dryout durations. In general, the sheath integrity could be impacted by:

- 1- The material failure stress, which mainly depends on:
 - (a) the sheath temperature, and
 - (b) the metallurgical structure (i.e., alpha-phase Zircaloy-4, prior β -phase Zircaloy-4, a combination of the two phases, and Zircaloy oxidation).
- 2- The sheath diameter and thickness.
- 3- The pressure difference across the sheath, which is the main driving force for sheath strain.
- 4- The sheath heating rate (for temperature ramp experiments) or the heating time (for isothermal holding experiments) which affects the sheath creep deformation.

1.1 Experimental burst curves

The previous factors form the basis of the sheath "Burst Curve", which is a relationship between the burst pressure difference and the burst temperature. Figure 1 shows the burst curves corresponding to the temperature ramp experiments listed in Table 1. This figure shows that, in general, for the same heating rate, the increase in the pressure difference across the sheath results in higher sheath stress and causes failure at a lower temperature. However, for the same conditions, there are some discrepancies among the data that are mainly attributed to the experimental uncertainties (which are shown in Figure 1), the distance between the temperature measuring location and the burst location, and the variation in the heating rate during the experiment (i.e., the heating rates shown in Figure 1 represent the nominal values).

The effect of the testing environment (vacuum or steam) is shown in Figure 2(a) for heating rates of 25 K/s. The presence of steam, which results in sheath oxidation, did not significantly affect the burst curves for a heating rate of 25 K/s. The same insensitivity to oxidation effect was also observed for heating rates of 1 and 100 K/s.

Table 1: Summary of sheath failure experiments used in the current assessment

No.	Author(s)	Year	Test Type	Surrounding Environment	Specimen Condition	Sheath Outer Diameter (mm)	Sheath Thickness (mm)
1	D. G. Hardy [11]	1973	Temperature Ramp and Isothermal Holding	Vacuum	As-received 28-element fuel	15.27	0.38
2	Chung et al. [14]	1977	Temperature Ramp	Vacuum	As-received	10.9	0.635
3	Hunt and Foote [7]	1977	Temperature Ramp	Vacuum	As-received PWR fuel and 28-element fuel	12.7 &15.2	0.38 & 0.43
4	J. L. Ricard [15]	1977	Temperature Ramp	Vacuum	As-received 28-element fuel and Appendages and HAZ to 28-element fuel	15.245	0.443
5	Hunt and Newell [5]	1978	Temperature Ramp	Vacuum	As-received 28-element fuel	15.25	0.45
6	P. E. Hynes [16]	1978	Temperature Ramp	He	As-received 28-element fuel	15.24	0.42
7	Chapman et al. [17]	1979	Temperature Ramp	Steam	As-received PWR fuel	10.92	0.635
8	Sagat et al. [10]	1982	Temperature Ramp	Steam	As-received 28-element fuel	15.25	0.44
9	Erbacher et al. [18]	1982	Temperature Ramp	Steam	As-received PWR fuel	10.75	0.725
10	Rosinger and Ferner [2]	1986	Temperature Ramp	Inert gas and Steam	As-received 28-element fuel	15.2 to 15.22	0.42
11	Erbacher and Leistikow [19]	1987	Temperature Ramp and one Isothermal Holding test	Steam and Steam followed by reflood	As-received PWR fuel bundles	10.75	0.72
12	Sagat and Foote [20]	1977	Temperature Ramp and Isothermal Holding	Vacuum	Appendages and HAZ to 28-element fuel	15.27	0.38
13	Hunt and Newell [21]	1979	Temperature Ramp	Vacuum	HAZ 28-element fuel	15.25	0.45
14	Sagat et al. [22]	1981	Temperature Ramp	Vacuum	HAZ 28-element fuel	15.25	0.45
15	Nicholson [23]	1981	Temperature Ramp	Vacuum	One appendages plane to 28-element fuel	15.2	0.44
16	Sagat et al. [24]	1983	Temperature Ramp and Isothermal Holding	Steam	One plane of appendages to 28-element fuel	15.25 & 15.24	0.44
17	Stern Laboratories IBIF tests using 37-element fuel bundles	2004	Temperature Ramp	Steam and Water	37-element fuel bundles with all the appendages	13.12	0.38 (minimum)
18	Hynes [25]	1979	Isothermal Holding	Inert gas	Appendages to 28-element fuel	15.2	0.42
19	Sagat [26]	1984	Isothermal Holding	Steam	Appendages to 28-element fuel	15.24	Not available

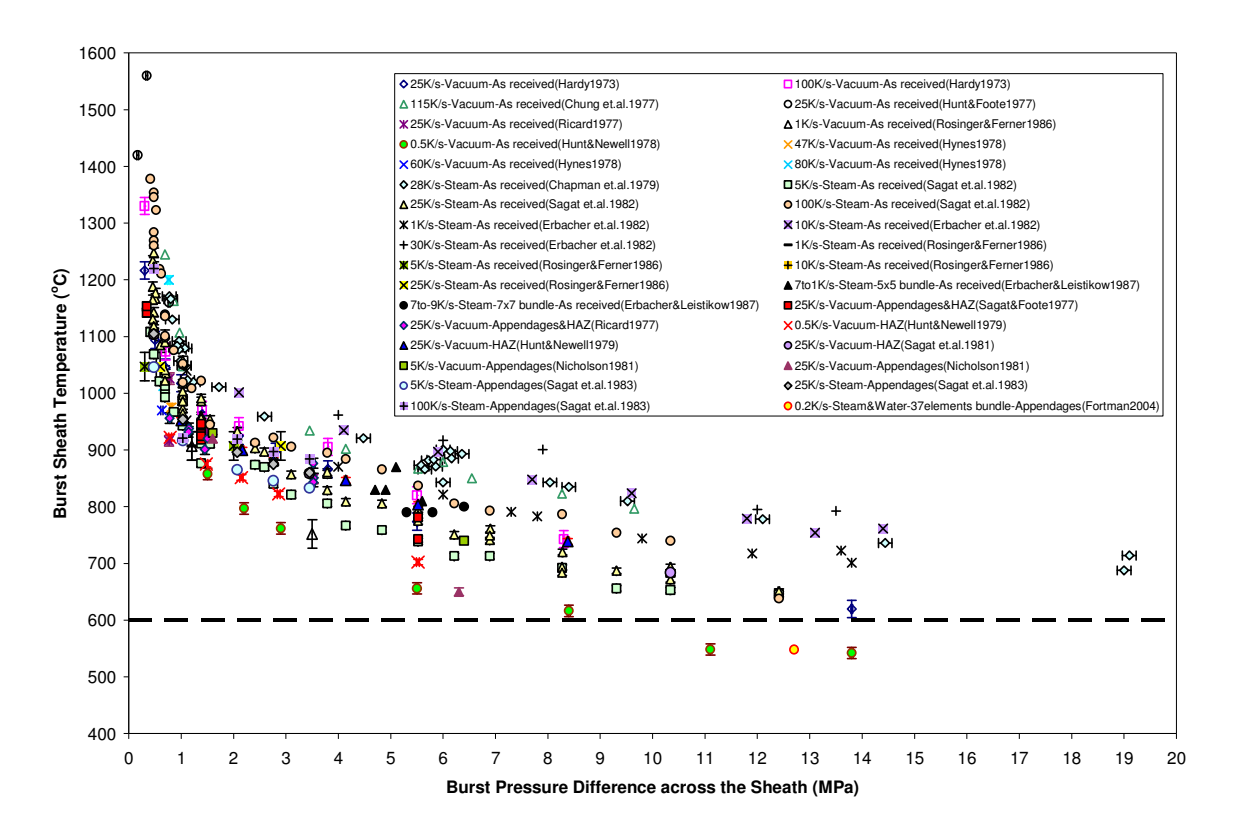


Figure 1: Burst curves for temperature ramp data using Zircaloy at different heating rates and test conditions

In Figure 2(b) the burst curves for as-received Zircaloy samples as well as samples with appendages are compared for a heating rate of 25 K/s in steam environment. The comparison shows that appendages do not affect the burst curves. The same insensitivity to the presence of appendages was also observed for lower heating rate of 1 K/s, however, for a heating rate of 100 K/s, appendages tend to shift the burst curve slightly downwards. This effect is relatively small and within the experimental discrepancy.

Recent measurements of the ultimate tensile strength of Zircaloy-2 (which almost has the same mechanical properties of Zircaloy-4) [4] showed that at 600°C the ultimate tensile strength significantly degrades with increase in temperature. Figure 1 shows that fuel sheath failure could occur at temperatures less than 600°C for relatively high pressure differences across the sheath (about 8.5 MPa or higher). This is evident from the data of Hunt and Newell [5] and Fortman [6] that used 28- and 37-element fuel sheaths, respectively. Therefore, limiting the sheath temperature to 600°C does not necessarily preclude fuel sheath failure for such experimental conditions.

The pressure difference across the sheath at burst conditions can be simplified as [7]

$$\Delta P \approx \frac{2\sigma t_i}{D_o - 2t_i} \tag{1}$$

where, $\Delta P = P_{gas}$ - $P_{coolant}$ = Pressure difference across the sheath,

 σ = Failure strength (a material property and is mainly a function of temperature),

 D_0 = Outer diameter, and

 t_i = Sheath thickness.

The 28- and 37-element fuel will have different burst curves because the 28-element has a larger outside diameter than the 37-element. For the same sheath thickness and sheath temperature (i.e., hence the same failure strength), Equation (1) indicates that the failure pressure difference of the 28-element will be lower than that for the 37-element fuel.

1.2 Experimental time-at-temperature fuel sheath failure maps

In order to study the combined effects of post-dryout duration (or the heating rate), sheath temperature, and the pressure difference across the sheath; time-at-temperature sheath failure maps were developed. The time-at-temperature fuel sheath failure map plots the relationship between the temperature and the time required to cause sheath failure at various pressure differences across the sheath (P_{gas} - $P_{coolant}$). Failure maps can be developed either directly or indirectly as follows:

- (1) Directly (using isothermal holding data): By isothermally heating the sheath in a gas or steam environment while keeping the pressure difference across the sheath constant and then recording the time (duration) to failure.
- (2) Indirectly (using the temperature ramp data): By using the burst curves at different heating rates, where for each pressure difference, the burst temperatures corresponding to the examined heating rates are obtained. Then, the post-dryout duration corresponding to each pressure and temperature is obtained by the following equation:

$$Post-dryout\ duration(s) = \frac{Temp.from\ the\ burst\ curve\ - Dryout\ Sheath\ Temp.}{Heating\ rate\ of\ this\ burst\ curve} \tag{2}$$

In the dryout experiments performed at Stern Laboratories for 28 and 37-element fuel, the onset of dryout was observed at sheath temperatures up to 370°C (References [8] and [9]). This temperature was used herein to develop the time-at-temperature fuel sheath failure maps using temperature ramp data. A sensitivity analysis was performed to investigate the impact of the assumed dryout sheath temperature on the failure maps by changing the dryout sheath temperature in range of 300 to 370°C and the impact was found to be insignificant.

Due to the scarcity of the 37-element experimental data, no experimental sheath failure map was developed for this type of fuel. The failure map based on 28-element fuel is expected to bound that for 37-element fuel for the same thickness and pressure difference, the diameter of the 37-element fuel sheath is smaller than that of the 28-element fuel sheath; hence, the resulting stresses are lower than those for 28-element fuel as indicated in Equation (1).

1.2.1 Failure maps using temperature ramp experiments

Selected burst curves for heating rates of 0.5, 5, 25, and 100 K/s were used to develop the temperature ramp experimental failure map. For the heating rates of 5 to 100 K/s, the data of Sagat et al. [10] for asreceived Zircaloy in steam environment were used. For the low heating rate of 0.5 K/s, the data of Hunt and Newell [5] for as-received Zircaloy samples in a vacuum were used because the effect of oxidation on the burst curve was shown to be insignificant as indicated in Figure 2(a).

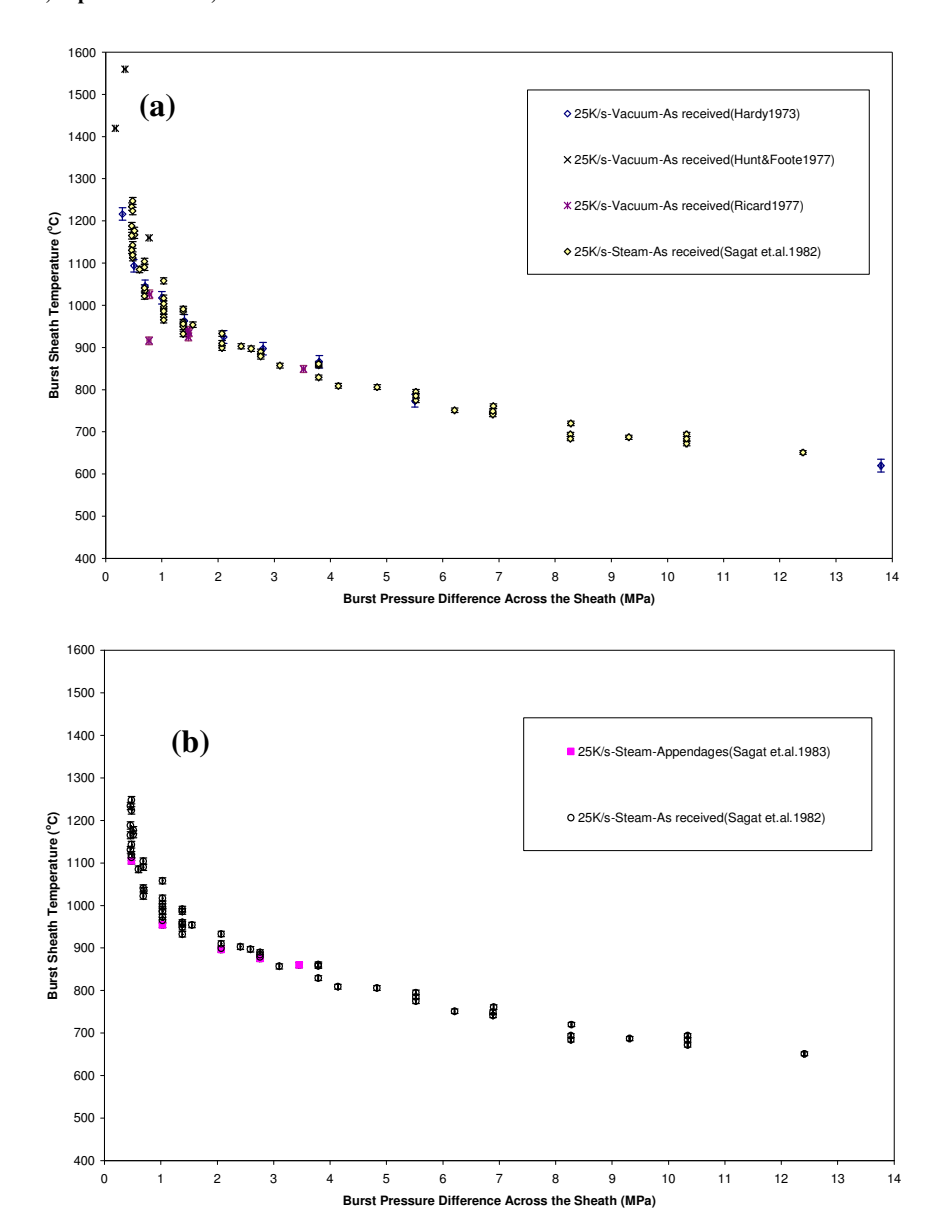


Figure 2: The effect of (a) steam oxidation and (b) appendages on the burst curve at heating rate of 25 K/s

Figure 3 shows the time-at-temperature sheath failure map based on the selected temperature ramp experiments. The pressure difference across the sheath affects the sheath failure time and temperature. Increasing the pressure difference at a given temperature results in earlier sheath failure. For the same post-dryout duration, increasing the pressure difference leads to sheath failure at lower temperature. The slope of the constant pressure difference curves in Figure 3 is high, thus, for the same pressure difference, a relatively small increase in the sheath temperature causes significant decrease in the failure time.

1.2.2 Failure maps using isothermal holding experiments

Figure 4 shows the time-at-temperature sheath failure map based on the isothermal holding experiments performed by Hardy [11]. These tests examined a wide pressure difference ranges. These

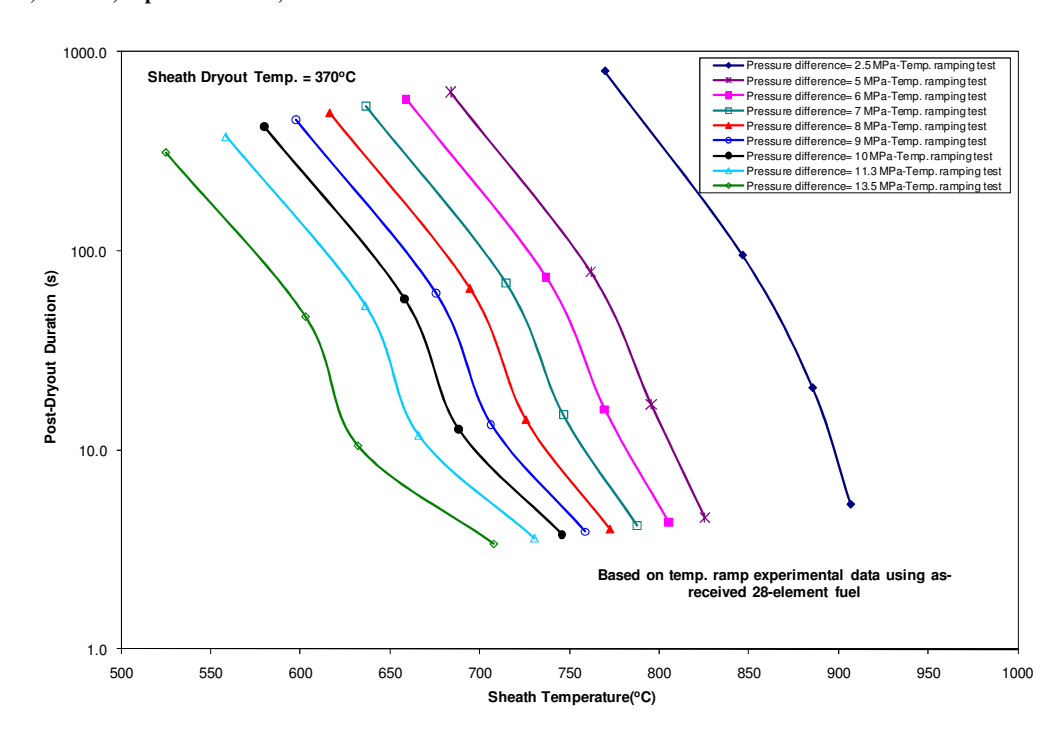


Figure 3: Experimental time-at-temperature fuel sheath failure map for 28-element fuel produced from temperature ramp experiments

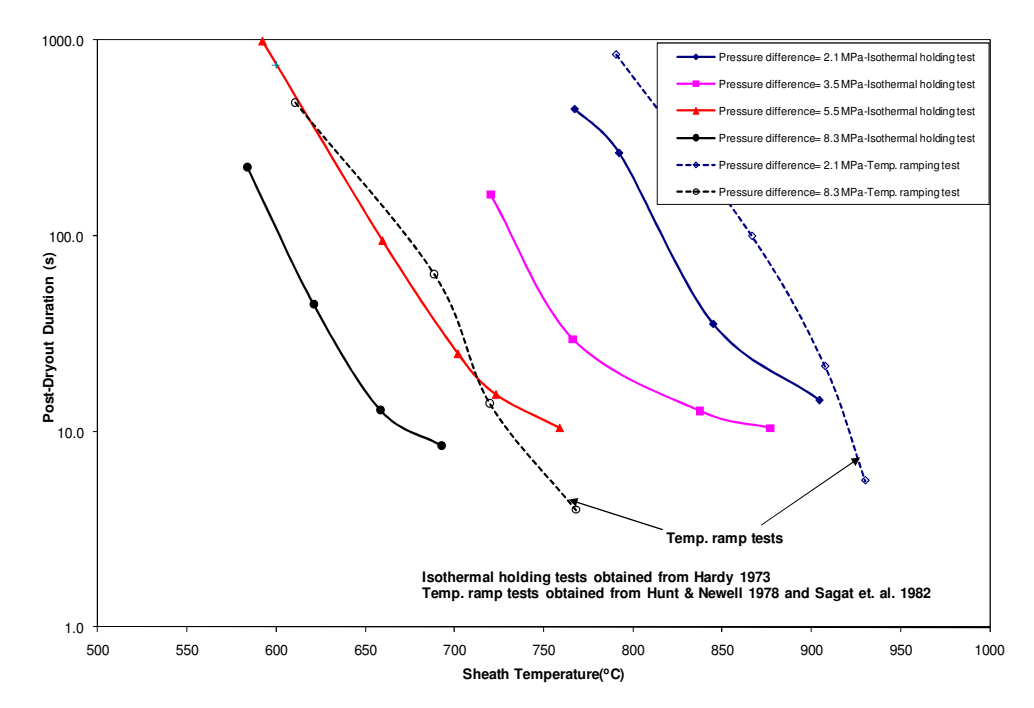


Figure 4: The time-at-temperature fuel sheath failure map produced from the isothermal holding experiments

experiments used as-received 28-fuel elements and were performed under vacuum conditions; however, the results can still be used for fuel elements under oxidizing conditions (as indicated in Figure 2(a)). For comparison, Figure 4 also shows some of the constant pressure difference lines obtained from the temperature ramp data. The failure maps based on isothermal holding data and temperature ramp data are generally consistent but the failure map based on the isothermal holding data is more conservative.

2. Analytical simulation for fuel sheath integrity

A number of simulations using the ELOCA 2.1c computer code [12] were performed to obtain analytical time-at-temperature sheath failure maps. ELOCA is a fuel analysis code used to simulate the thermo-mechanical response of the fuel elements during transient conditions. The fuel element was represented by one axial segment made of as-received Zircaloy-4 in steam environment. The sheath thickness was conservatively assumed to be equal to its minimum manufacturing value of 0.38 mm to maximize the rate of strain. Only the indirect method is used to obtain the analytical fuel sheath failure map (i.e., using ramp temperature simulations). The burst curves at different heating rates for the 28-and 37-element fuel were predicted using ELOCA and then Equation (2) was applied assuming dryout sheath temperature of 370°C. Five heating rates of 0.5, 1, 5, 25, and 100 K/s were examined. At a given heating rate, the initial internal gas pressure was varied from 0 to 20 MPa. The internal gas pressure, ranges from 14 to 20 MPa, was used to activate sheath failure by athermal strain that was not observed in the experiments. Urbanic-Heidrick correlation was used to model the oxidation kinetics [13]. The following sheath failure mechanisms and failure limits were considered during ELOCA simulations:

- Sheath failures due to sheath overstrain using a failure limit of 5%.
- Sheath failures due to Beryllium assisted crack penetration (BACP), which occurs when the failure probability exceeds 95%.
- Sheath failures due to athermal strain, which occurs when the athermal strain reaches 0.4% and the volume fraction of the re-crystallized alpha-Zr-4 phase is more than 95%.
- Sheath failures due to oxygen embrittlement occur during quench when the oxygen concentration at the sheath mid-plane exceeds 0.7wt%.

Figures 5 and 6 show the analytical time-at-temperature fuel sheath failure maps for the 28- and 37-element fuel bundles, respectively. Figure 5 also shows a comparison between the failure curves obtained from ELOCA simulations and those obtained from the experimental ramping data at 2.5 and 13.5 MPa (from Figure 3). The analytical curves are more limiting than the experimental ramping data. This conservatism is considered to a consequence of the approaches and assumptions used in ELOCA calculations (e.g., setting conservative sheath failure limits). Figure 6 shows a comparison between the 28- and 37-element failure maps for selected pressure differences of 2.5 and 13.5 MPa. It is evident from the figure that the 28-element curves are more limiting due to the effect of the larger sheath diameter discussed earlier.

3. Applying failure maps to predict fuel sheath integrity

Time-at-temperature sheath failure maps can be used as a simple and effective method to demonstrate the fuel sheath integrity during a postulated design basis accident upon by examining the sheath temperature at reactor trip, the pressure difference across the sheath at the trip time, and the time for the onset of sheath dryout (the dryout duration can be determined by subtracting the onset dryout time from the trip time). Then by locating the derived point on the failure map and comparing it to the constant pressure difference curve, one of the following cases would apply:

- If the point is located under the constant pressure curve corresponding to the pressure difference at time of trip, the sheath failure is precluded.
- If the point is located above, or at, the constant pressure curve, there is a potential for sheath failure. In this case, the possibility of failure or no-failure will be dependent on the accuracy of the selected map to be used such as the uncertainty of the experimental data (in case of using the

experimental failure maps) the assumed dryout temperature, the accuracy and conservatism in the assumptions used to develop (in case of using the analytical maps).

In the second case, further detailed analysis for fuel sheath integrity could be required for confirmation.

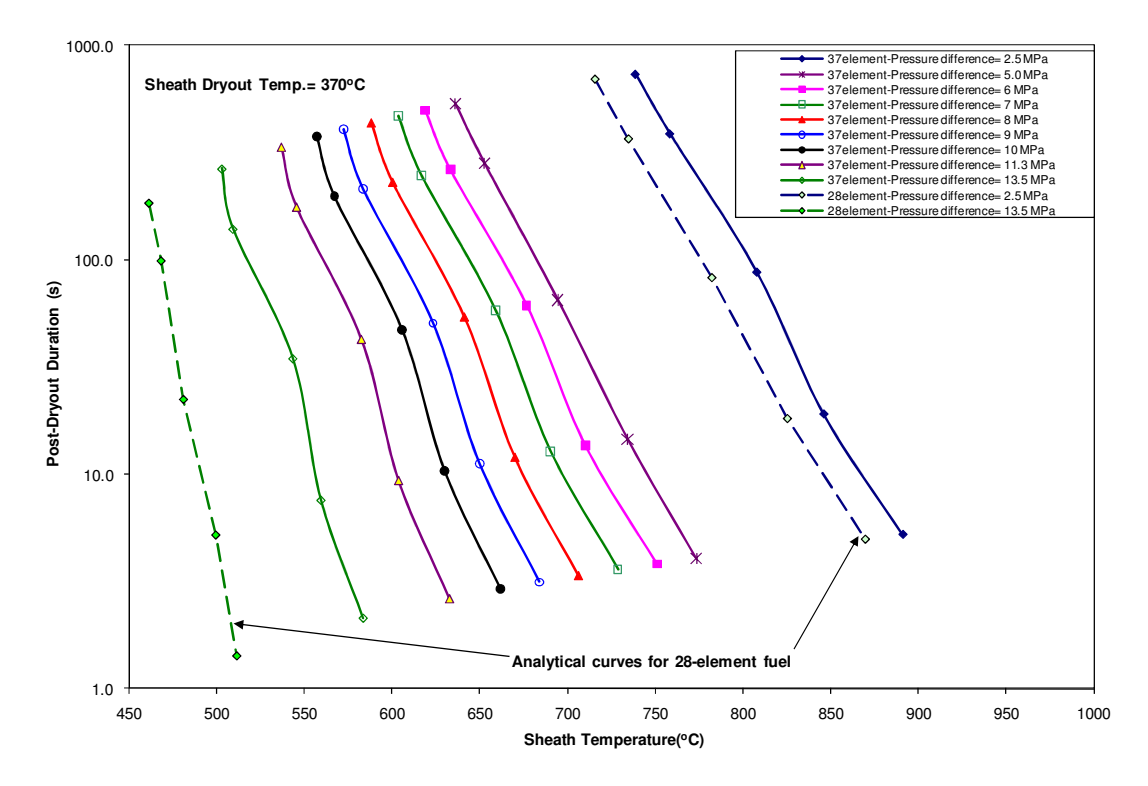


Figure 5: The analytical 28-element time-at-temperature fuel sheath failure map (For comparison, additional curves from the experimental failure map are also shown (i.e., from Figure 3))

4. Conclusions

A technical assessment of CANDU fuel sheath integrity during post-dryout operation was performed by reviewing the available experimental data that investigated the fuel sheath integrity. Additional simulations using ELOCA code were performed to investigate the fuel sheath integrity under extended conditions that were not fully covered by experiments. The assessment examined the following sheath failure mechanisms:

- Sheath overstrain due to ballooning,
- Beryllium assisted crack penetration (BACP), and
- Athermal strain.

Fuel sheath integrity during post-dryout operation was found to be primarily dependent on three key factors: the pressure difference between the fuel element internal gas pressure and the surrounding coolant, the post-dryout sheath temperature and the post-dryout duration. Conservative time-attemperature fuel sheath failure maps have been developed based on the review of existing experimental work, and the performed analytical studies. The maps identify the boundary of fuel failure-no fuel failure using the three key factors. Maps are produced for both the 28- and 37-element fuel bundles. The maps show that the pressure difference across the fuel sheath plays a major role in fuel sheath

failure. The developed time-at-temperature sheath failure maps can be used as a simple and effective method to demonstrate the fuel sheath integrity during a postulated design basis accident.

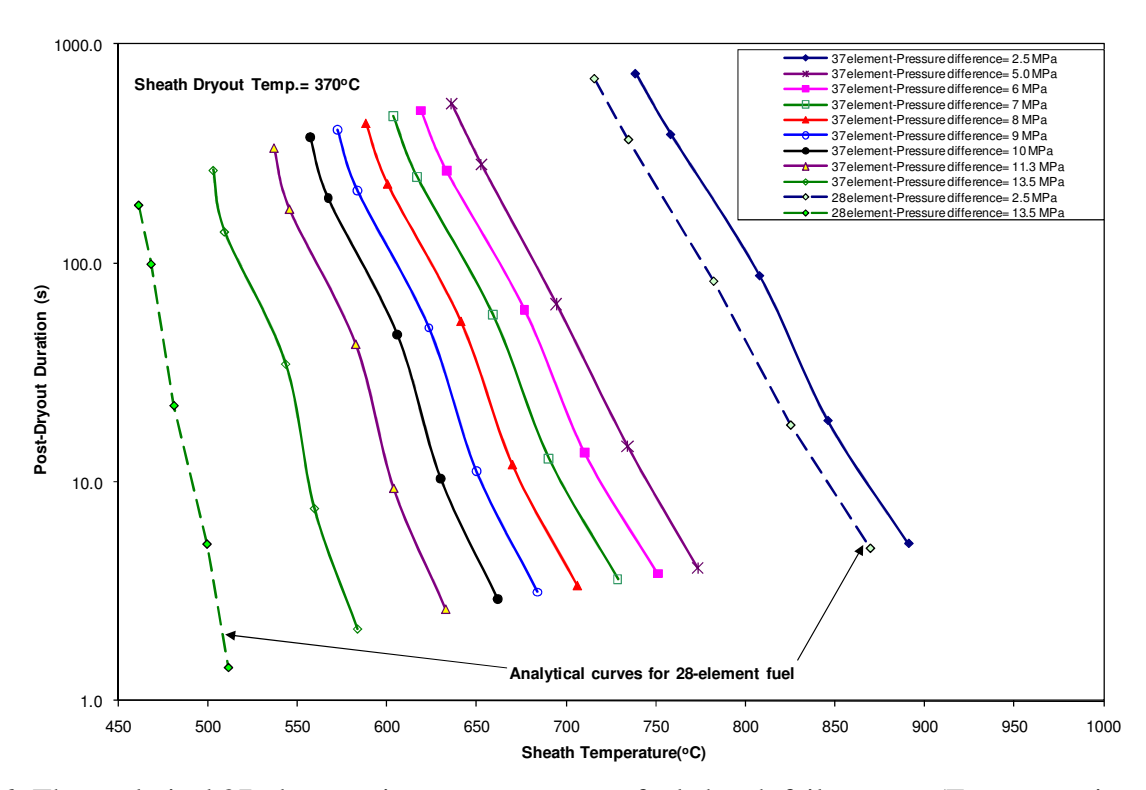


Figure 6: The analytical 37-element time-at-temperature fuel sheath failure map (For comparison, additional curves from the 28-element analytical failure map are also shown (i.e., from Figure 5))

5. References

- [1] A.F. Williams, "Implementation Of Sheath Failure Mechanisms in ELOCA Code", CANDU Owners Group, OP-08-2117, 2008, December.
- [2] H.E. Rosinger and J. Ferner, "A Study of the Effect of Circumferential Temperature variation on Fuel-Sheath Failure", Research mechanics, Vol. 19, 1986, pp. 143-161.
- [3] H.E. Sills and R.A. Holt, "NIRVANA, a High Temperature Creep Model for Zircaloy Fuel Sheathing", AECL Report AECL-6412, 1797, May.
- [4] B.S. Rodchenkov and A.N. Semenov, "High temperature mechanical behavior of Zr–2.5% Nb alloy", Nuclear Engineering and Design, Vol. 235, 2005, pp. 2009-2018.
- [5] C.E.L. Hunt and W.G. Newell, "The Ballooning Behaviour of Zircaloy-4 Fuel Sheaths at a Heating Rate of 0.5°C·s⁻¹", AECL Report, AECL-6342, 1978.
- [6] R.A. Fortman, "Results of commissioning tests performed in the new IBIF test facility with a pressurized element", CANDU Owners Group, Technical Note, TN-03-2101, 2004. July.
- [7] C.E.L. Hunt and D.E. Foote, "High Temperature Strain Behavior of Zircaloy-4 and Zr-2.5Nb Fuel Sheaths", <u>Proceeding of the 3rd International Conference of Zirconium in Nuclear Industry</u>, 1977, pp. 50-65.
- [8] R.A. Fortman, and J. Snell, "PDO and CHF Tests on CANDU 28-Element Fuel (Interim Report)", CANDU Owners Group, COG-07-2109, 2007.

- [9] R.A. Fortman, R.C. Hayes, and G.I. Hadaller, "37-Elements CHF Program Steady-State CHF, Transient CHF and Post Dryout Tests with Uniform and Diametral Crept Flow Tubes", CANDU Owners Group, COG-98-311, 1999.
- [10] S. Sagat, C.A. Wills, J.A. Walsworth and D.F. Shields, "Rupture Behaviour of Internally Pressurized Zircaloy Fuel Sheathing Tested at Constant Heating Rates in a Steam Atmosphere," AECL Report CRNL-2385, 1982, September.
- [11] D.G. Hardy, "High Temperature Expansion and Rupture Behaviour of Zircaloy Tubing", National Topical Meeting on Water Reactor Safety, Salt Lake City, Utah, CONF-730304, 1973, pp. 254-273.
- [12] A.F. Williams and H.M. Nordin, "ELOCA-IST 2.1 Users' Manual", CANDU Owners Group, COG-00-274, 2001, August.
- [13] V.F. Urbanic and T.R. Heidrick, "High-Temperature Oxidation of Zircaloy-2 and Zircaloy-4 in Steam", Journal of Nuclear Materials, Vol. 75, 1978, pp.251-261.
- [14] H.M. Chung, A. M. Grade, and T. F. Kassner, "Deformation and Rupture Behavior of Zircaloy Cladding under Simulated Loss-of-Coolant Accident Conditions", <u>Proceeding of the 3rd International Conference of Zirconium in Nuclear Industry</u>, 1977, pp. 82-97.
- [15] J.L. Ricard, "Strains and Rupture Behaviour of Internally Pressurized Zircaloy-4 Fuel Sheaths Under Transient Temperature Conditions by an Internal Heater", Canadian General Electric Ltd. Report R77CAP1, 1977, March.
- [16] P.E. Hynes, "1978 Sheath Strain Model Verification Test Results", Canadian General Electric Ltd. Report CGE-R79CAP1, 1979, January.
- [17] R.H. Chapman, J.L. Crowley, A. W. Longest, and G. Hofmann, "Zirconium Cladding deformation in a Steam Environment with Transient Heating", <u>Proceeding of the 4th International Conference of Zirconium in Nuclear Industry</u>, 1979, pp. 393-408.
- [18] F.J. Erbacher, H.J. Neitzel, H. Rosinger, H. Schmidt, and K. Wiehr, "Burst Criterion of Zircaloy Fuel Cladding in a Loss-of-Coolant Accident", <u>Proceeding of the 5th International Conference of Zirconium in Nuclear Industry</u>, 1982, pp. 271-283.
- [19] F.J. Erbacher and S. Leistikow, "Zircaloy Fuel Cladding Behaviour in a Loss-of-Coolant Accident: A Review", <u>Proceeding of the 7th International Conference of Zirconium in Nuclear</u> Industry, 1987, pp. 451-488.
- [20] S. Sagat and D.E. Foote, "High-Temperature Strain Behaviour of Zircaloy Fuel Sheaths with Be-Brazed Appendages", AECL Report CRNL-1605, 1977, September.
- [21] C.E.L. Hunt and W.G. Newell, "Effect of β-Phase Heat Treatment on the Subsequent α-Phase Ballooning Behavior of Zircaloy-4 Fuel Sheaths", <u>Proceeding of the 4th International Conference of Zirconium in Nuclear Industry</u>, 1979, pp. 447-464.
- [22] S. Sagat, D.C. Hardy, and D.E. Foote, "High Temperature Ballooning of Braze-Cycled Zircaloy-4 Fuel Sheathing," AECL Report CRNL-2150, 1981, January.
- [23] A.M. Nicholson, "Effects of Constrained Appendages on Behaviour of Fuel Sheaths during a High Temperature Transient", Canadian General Electric Ltd. Report, CGE-R80CAP14, 1981, July.
- [24] S. Sagat, D. Lim and D.E. Foote, "Rupture Behaviour of Zircaloy-4 Fuel Sheaths with Brazed Appendages in a Steam Atmosphere", AECL Report CRNL-2418, 1983, June.
- [25] P.E. Hynes, "Test Results of Appendaged Fuel Sheath Specimens Heated by Indirect Internal Heating to Verify Beryllium Assisted Crack Penetration Formulae", Canadian General Electric Ltd. Report ITD 66-28-79, CANDEV 97-05, 1979, April.
- [26] S. Sagat, "Effect of restraint on Rupture Time in Be-Brazed Failures", Memorandum, AECL, CRNL-83393, 1984, May.